# A Tough and High-Performance Transparent Electrode from a Scalable and Transfer-Free Method

Tianda He, Aozhen Xie, Darrell H. Reneker, and Yu Zhu*

Department of Polymer Science, College of Polymer Science and Polymer Engineering, The University of Akron, 170 University Circle, Akron, Ohio 44325-3909, United States

ABSTRACT Conductive metal films are patterned into transparent metal nanowire networks by using electrospun fibers as a mask. Both the transmittance and sheet resistance (6 $\Omega/\square$ at 83% transmittance and 24 $\Omega/\square$ at 92% transmittance) of the metal nanowire-based electrode out-perform commercial indium doped tin oxide (ITO) electrodes. The metal nanowire-based transparent electrodes were fabricated on both rigid glass and flexible polyethylene terephthalate (PET) substrates. In addition to state of art performance, the transparent electrodes also exhibit outstanding toughness. They can withstand repeated scotch tape peeling and various bending tests. The method for making the metal nanowire is scalable, and a touch screen on flexible substrate is demonstrated.
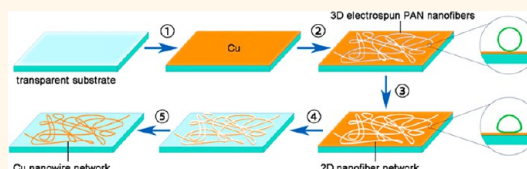
Transparent electrodes are essential parts for many optoelectronic devices such as touch screens, liquid crystal display, and solar cells. Currently, commercial transparent electrodes are made from indium doped tin oxide. The cost of indium and the brittle nature of ITO drive the search for alternative transparent electrode materials. During the past decade, many alternative transparent electrode materials were studied, for instance: conducting polymers,[1] graphene,[2−4] carbon nanotube (CNT),[5,6] metal nanowire,[7−12] and hybrid materials.[13−16] Those materials can be categorized into two forms: the continuous transparent conductive film (graphene, ITO and conducting polymer) and transparent percolation-conductive film (CNT, metal nanowire and hybrid materials). In continuous transparent conductive materials, graphene has highest carrier mobility[17] and optical transparency.[18] Such performance is only available on small, nonscalable mechanically cleaved graphene.[19] The large graphene samples from other sources, such as chemical vapor deposited graphene[2,3] and solution-processed, reduced graphene oxide,[20] cannot provide comparable perfection (carrier mobility) as small cleaved graphene.[19] The carrier mobility in large area graphene samples is limited by the production techniques, so doped graphene was developed by several groups[21−23] to enhance the conductivity by increasing the carrier density. Some doped graphene-based transparent electrodes exhibit performance similar to ITO.[21] The doped graphene sheets are less stable than the pristine graphene and the fabrication cost are likely to be larger. The high processing cost (such as chemical vapor deposition) and tedious transferring processes hinder its use in transparent electrodes. As a result, ITO is presently the best choice for continuous transparent electrode materials due to its combined properties of performance, cost, stability, and toughness. The transparent percolation-conductive film is another emerging material for making high-performance transparent electrodes.[5−16] In contrast to continuous transparent conductive film, the transparent percolation-conductive film can be made from opaque materials such as carbon nanotubes (CNTs) and metal nanowires. Carbon nanotubes are used to make transparent electrodes because of their extremely high conductivity and aspect ratio. The transparent electrodes made of CNTs are poorer than ITO due to the presence of semiconductive single-walled carbon nanotubes and high contact resistance.[5,6] Metal nanowire transparent
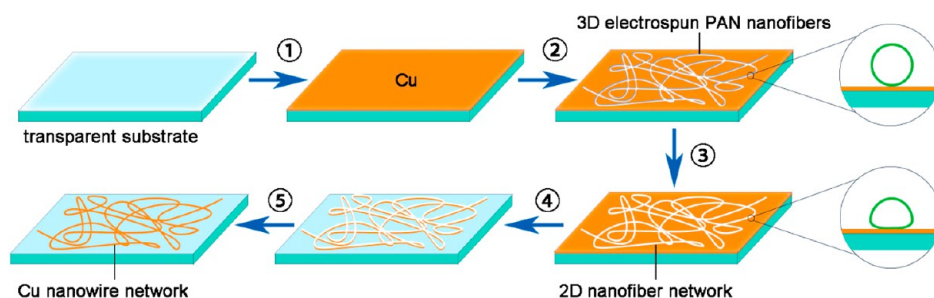
Figure 1. Scheme of copper nanowire network electrode fabrication. (1) Electron-beam deposition of copper film on the transparent substrate. (2) Electrospin PAN nanofibers on the copper-covered substrate. (3) Solvent vapor annealing. The insets show the schematic fiber cross-section shapes before and after solvent vapor annealing. (4) Metal etching. (5) Removal of PAN fibers by dissolution.

electrodes emerge as better transparent electrodes than CNT electrodes.[7−16] The best solution-processed copper nanowire[11] and silver nanowire[7−9] based electrodes exhibit better performance than ITO. However, the solution-processed metal nanowires often contain organic residues that result in lower conductivity in comparison with that of patterned metal nanowire made from evaporated metal.[14,24] Recent research[7] also indicates that solution-processed metal nanowire transparent electrodes may have poor adhesion[25,26] and protrusions[12] that limit their use in many devices.

Patterned metal nanowires from evaporated metal sources exhibit the best transparent electrode performance.[14,24] However, a high throughput patterning method to generate the high aspect ratio nanowires are crucial for this type of transparent electrode. Electrospinning is a facile and economical way to produce continuous nanofiber structures. Previously, it was used to generate continuous conductive nanofibers for transparent electrodes.[10,27] The directly electrospun conductive nanofibers are usually polymer−metal composites. A heat treatment annealing process is required to eliminate the organic residue and obtain reasonable conductivity. This process is not only energy and time-consuming but also limited to substrates that are stable at high temperatures. Cui's group coated metal on continuous electrospun fibers. The small diameter and ultralong fiber lead to a metal nanotrough network electrode with remarkable performance (sheet resistance 2 Ω/□ at 90% transmittance).[24] However, the metal nanotrough network needs to be transferred onto the target substrate, which generates defects and requires additional care to ensure adhesion. In our previous work,[14] we demonstrated that a patterned metal mesh with graphene can provide excellent transparent electrode (sheet resistance 20 Ω/□ at 91% transmittance).[14] This method involves expensive photolithography. It is presently a challenge to fabricate transparent electrodes with high performance, low cost, and high throughput that can replace ITO.

RESULTS AND DISCUSSION

In this work, the electrospun fibers are used as a mask to create metal nanowires on transparent substrates.

The fabrication procedure is illustrated in Figure 1. First, the conductive metal film is deposited on the transparent substrates such as glass or transparent polymer sheets. Second, polyacrylonitrile (PAN) fibers are electrospun onto the surface of the metal film. In the third step, a solvent annealing process is conducted to flatten the PAN fibers onto the metal surface. Then in step four, the coated transparent sheet is immersed into a metal etching solution to remove the metal that is not protected by the PAN fibers. Finally, the PAN fibers are removed by an organic solvent, and the transparent electrode is ready to be tested and used.

Copper is the metal of choice in this work because of its high conductivity and low cost. In a typical case, a 2 nm thick layer alumina (Al_2O_3) and a 100 nm copper layer are deposited in that order on glass slides by electron-beam evaporation in series. The Al_2O_3 is used as an adhesive layer to enhance the adhesion between the copper film and glass substrate. Electrospun nanofiber networks provide percolating paths, even when the number of fibers per unit area is small. The electrospun fiber network is formed by very long continuous fibers. The resulting metal nanowire patterns are therefore completely connected everywhere. In contrast, unconnected nanowires or nanotubes are often found in CNT or solution-processed metal nanowire electrodes. Such isolated nanowires/nanotubes reduce transmittance without enhancing conductivity. Second, electrospinning is the best technique that provides small feature with high manufacturing rate per unit area. Lithography techniques such as nanoimprinting[28] and e-beam lithography can generate even smaller nanowires than electrospun fibers, but they require expensive instruments and have limited productivity. Conventional photolithography and shadow-mask patterning can provide metal wire patterns with relatively high throughput, but the widths of the metal wires are usually larger than a micrometer. In transparent percolation electrode, the aspect ratio of length of metal nanowires vs the diameter and the number of the nanowires determines the performance. Electrospinning leads to high conductivity networks and easy optimization of the balance of the length between connection points, cross sectional area of the
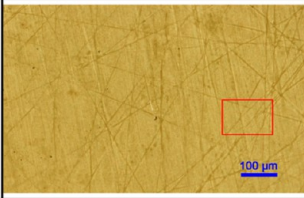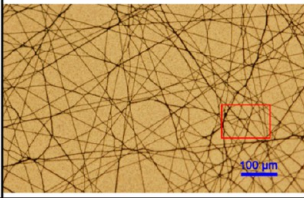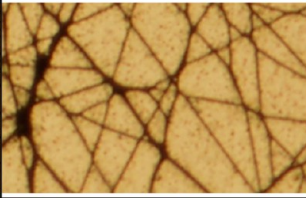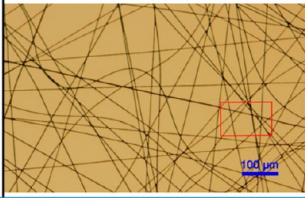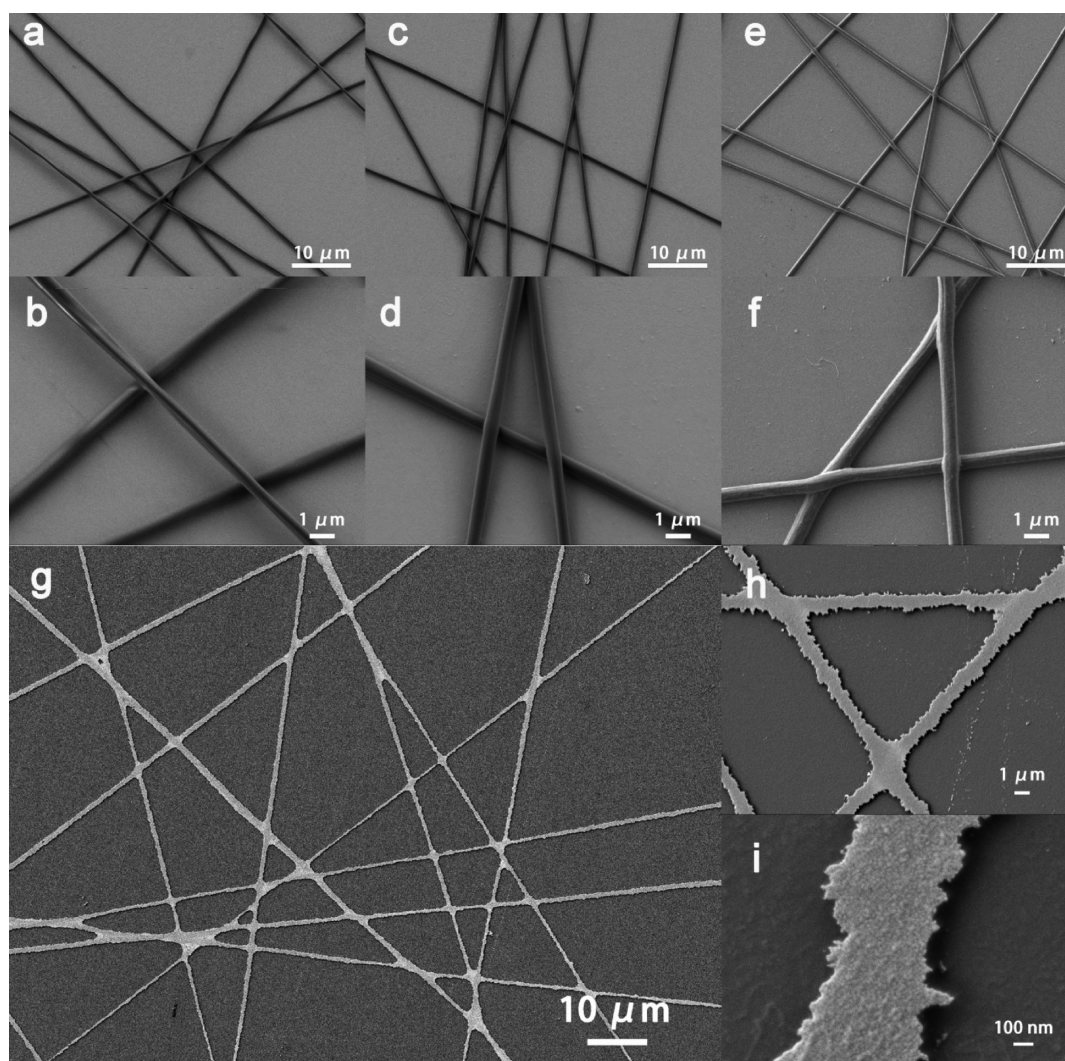
Figure 2. Scanning electron microscope (SEM) images of patterned transparent substrates made as described in this paper. (a,b) The as prepared electrospun PAN fibers on the copper-coated glass substrate. (c,d) Solvent vapor annealed PAN fibers on the copper-coated glass substrate. (e,f) The copper wire with PAN fiber on the glass substrate after rinsing etching. (g−i) Copper nanowire network on transparent substrate after PAN is removed. Panel (i) shows the width of the copper nanowire.

metal conductor, and number of conducting segments per unit area.

The scanning electron microscope (SEM) images of the as prepared PAN fiber on copper substrates are shown in Figure 2a,b. The diameter of the PAN fiber in this work is typically between 650 and 700 nm. Initial etching experiments without solvent softening of the PAN nanofibers did not protect the copper. The as prepared fibers stacked with each other, and many segments did not contact the copper surface directly.[29] From Figure 2b, it is clear the one fiber is suspended above the other two. In order to transfer the PAN nanofiber pattern to the copper layer, all PAN nanofibers need to contact the copper surface. Therefore, a solvent wetting process was used in this work. The experimental setup is illustrated in Supporting Information (SI) Figure S1. DMF was heated by a water bath (75 ± 5 °C), and the vapor was guided by an air

stream to a glass funnel directly above the sample. The wetting level should be controlled accurately in order to obtain optimal contact between with the fibers and the copper surface without distorting the shape of the fibers. In our experiments, the wetting time was typically between 1 and 3 min with an air flow rate of 750 mL/min. After the samples were treated by this wetting process, most segments of the PAN fibers contacted the copper surface (Figure 2c,d). In addition, the junctions of the fibers are conglutinated (Figure 2c,d). Although the sizes of the final copper nanowire are theoretically controlled by both wetting procedure and the following etching procedure, it was found in this work that the control of the wetting was a lot easier. Figure S2 in the Supporting Information shows that the stepwise wetting gradually changed transmittance from 60 to 90%.

TABLE 1. Comparison of Different Etching Methods and the Resulting Nanowire Pattern

Etching methods	Etching time	Optical images	
Static soak etching	>30 min		
Stirring etching	5 min		
Rinsing etching	<2 min		

Another key step in this work is the wet-etching process. The wet-etching of copper is an anisotropic process; therefore, undercutting is typically observed during the process. When the feature size is close to a micrometer, undercuts become a serious problem. When the diameters of electrospun fibers are all under a micrometer, conventional static soaking methods do not work well. As shown in Table 1, it was almost impossible to prepare samples at a size of 2.54 × 2.54 cm by static soaking. This undercut problem was not solved by using copper etchants with different concentration ($FeCl_3$ 0.001−0.1 M) or different etchants ($FeCl_3$,[30] $(NH)_4S_2O_8$,[31] and $CuSO_4+H_2SO_4$[14]). A rinsing etching method was adopted (see Methods and SI Figure S2). The agitation of etching solution (stirring etching) helped to suppress undercutting by rapidly exchanging the etching solution on the metal surface. The etching time and results of the static soaking, stirring, and rinsing etching are listed in Table 1.

From the optic images, it is clear that that the static soak etching did not give any useful patterning because of the undercut effect. The stirring etching (using a magnetic stir-bar to agitate the etching solution) formed nanowires pattern, but residues were left in the open areas. The rinsing etching (see Methods and SI Figure S3) generated well patterned fiber networks with clean background.

With optimized rinsing etching condition, the pattern of the PAN nanofibers was reproduced in the copper substrate. Figure 2e,f shows that the PAN fibers protected the underlying copper substrate during rinsing etching, while the copper in the exposed region was removed completely. SEM EDAX mapping (SI Figure S4) clearly indicated the copper nanowires are well patterned under the polymer fibers. Figure 2g−i shows SEM images of the final copper nanowire on the glass substrate after the PAN was removed by hot DMF. The copper nanowire had widths between 550 and 800 nm, which are very close to the diameters of PAN nanofibers. It is worth emphasizing that the rinsing etching is an efficient and reliable method to produce transparent metal nanowire electrodes with yields over 90%.

Copper nanowire transparent electrodes are shown in Figure 3. Figure 3a shows four 2.54 × 2.54 cm size transparent electrodes on glass substrates. They exhibit transmittance from 68 to 90% (at 550 nm). The sheet resistance was between 2 and 24 Ω/□. The transmittance of the electrode is mostly controlled in the wetting step. The samples with 68, 74, 83% transmittance were obtained from a 100 nm thick copper film on the glass. The sample with 90% transmittance was obtained from a 50 nm thick copper film on the glass. (SI Figure S5). The transparent electrodes show similarly high transmittance throughout the wavelength range between 400 and 800 nm.

This method was used to fabricate flexible transparent electrodes. The only change required is to use polyethylene terephthalate substrate to replace glass substrate. Copper nanowire-based flexible transparent electrode was fabricated with high yield. Figure 3c
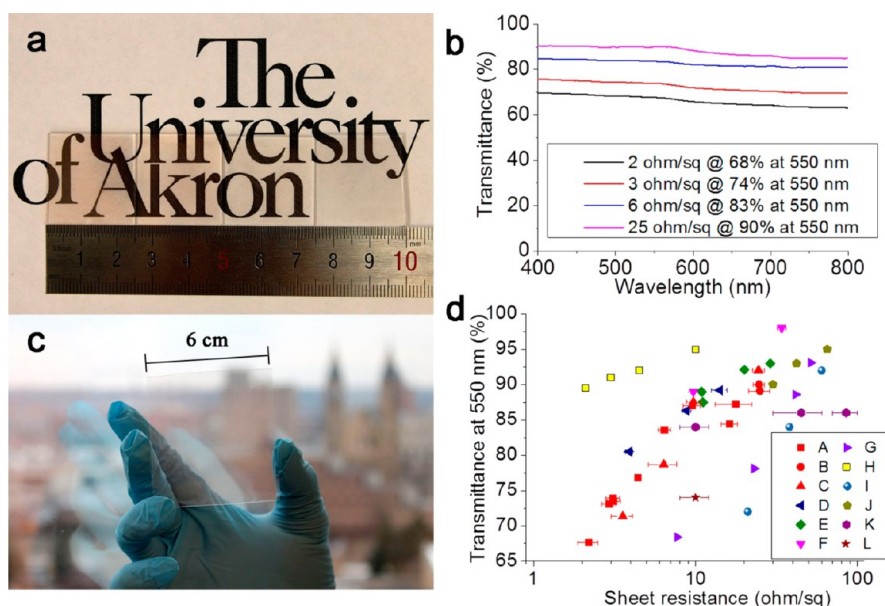
Figure 3. (a) Photograph of 2.54 × 2.54 cm copper nanowire transparent electrode on glass substrates with sheet resistance of 2, 3, 6, 25 Ω/□ and transmittance at 550 nm 68, 74, 83, 90%, from left to right, respectively. (b) The transmittance of the transparent electrodes shown in (a) at the wavelength between 400 and 800 nm. (c) A 6 × 6 cm flexible copper nanowire transparent electrode. (d) Sheet resistance *vs* transmittance figure of different transparent electrode from commercial source and literatures. A−C: the transparent electrodes from this work with 100 nm thick copper nanowire on glass, 50 nm thick copper nanowire on glass, and 60 nm thick copper nanowire on PET, respectively. D,[7] E,[8] F:[9] silver nanowires. G: copper nanowires.[11] H: copper nanotrough.[24] I: CNT.[6] J: graphene.[21] K: commercial ITO on glass.[32] L: commercial ITO on PET.[32]

shows a 6 cm × 6 cm flexible transparent electrode. The sheet resistance and transmittance of the rigid and flexible transparent electrodes prepared in this work are plotted in Figure 3d. The reported sheet resistances are average values of 10 measurements. The variation is reported in Figure 3d, which shows the recent reports of transparent electrodes research. The performance of the transparent electrodes fabricated in this work is better than ITO,[32] CNT,[6] and graphene-based electrodes.[21] The result is also better than the solution-processed copper nanowire[11] and comparable with the best results of solution-processed silver nanowire transparent electrodes.[7−9] Although the diameters of the solution-processed copper nanowire[11] are smaller, the transparent electrodes from them are less conductive. The performance of the transparent electrodes in this work is comparable with our previous work.[14] However, the previous work requires expensive photolithography tools.[14] The metal nanowires from photolithography are much larger (>2 μm), which requires a coarser grid (200 μm) to reach high transparency. In this work, the copper wires (avg. ~650 nm) were much smaller and were fabricated at a higher rate per unit area. Recent work[24] used evaporated metal and electrospinning methods with good results because the width of electrospun fibers was smaller (245 nm in that work *vs* 650 nm in this work). However, the free-standing metal nanotrough needs to be transferred and adhered to other substrate, which increases the fabrication cost. In this work,

no transfer process is required because the transparent electrodes are directly formed on the transparent substrate. We expect that if the smaller electrospun fibers are used in the process described here, better properties will be obtained. Nevertheless, the figure of merit result based on the percolation theory[33,34] (SI Figure S6 and Table S1) indicates that our results are certainly among the best reports for metal nanowire-based transparent electrode.

In addition to the excellent transmittance and conductivity, the transparent electrodes in this work exhibit outstanding toughness. The transparent electrodes were evaluated in various bending tests and adhesion tests. In the bending test, the flexible transparent electrode was fixed between two clamps and then bent by pushing the two clamps together (Figure 4a). The resistance of electrodes was measure throughout the test and did not change over 10% when the bending radius changes from 51 to 1.25 mm (Figure 4b). In comparison, previous copper nanotrough electrode[24] was bent up to 2 mm radius, and the resistance of silver nanowire electrode[7] changed ~16% when the bending radius is 1.3 mm. The bending radius is calculated using the following equation:

$$\begin{cases} \dfrac{d}{2r} = \sin\left(\dfrac{L}{2r}\right) & \left(d > \dfrac{2l}{\pi}\right) \\ r = \dfrac{d}{2} & \left(d < \dfrac{2l}{\pi}\right) \end{cases} \qquad (1)$$
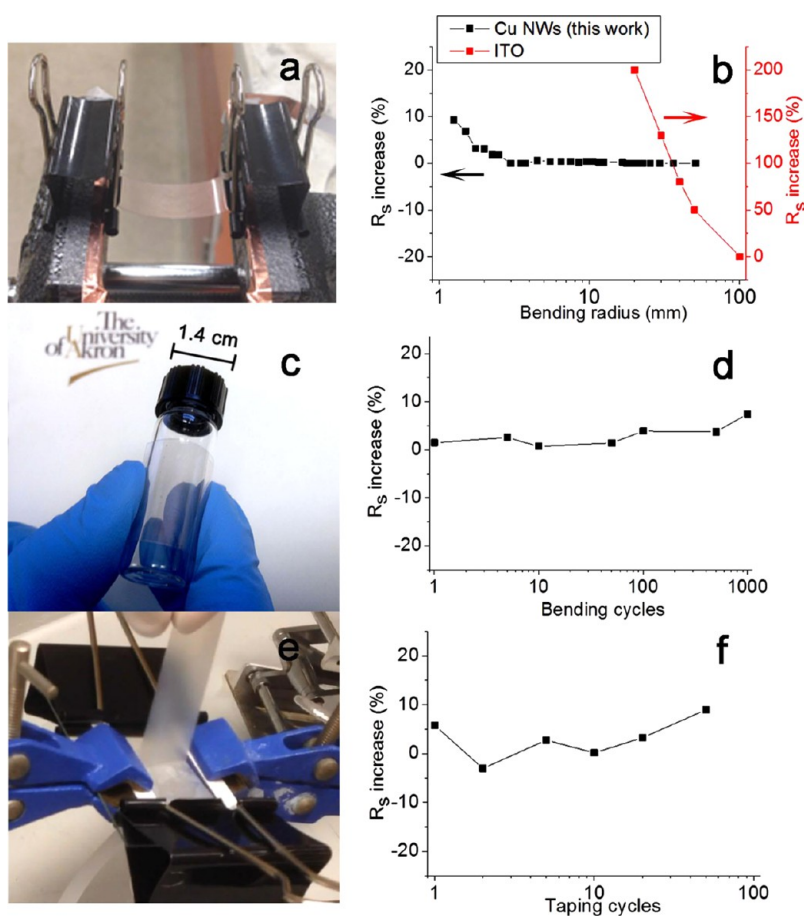
Figure 4. Bending and taping tests results of transparent electrode. (a) Bending test setup. The copper nanowire on PET was clamped and bent by pushing the two ends together. (b) Sheet resistance changes *versus* bending radius. (c) Flexible Cu nanowire electrodes on PET bent on a 14 mm vial. (d) Sheet resistance changes *versus* number of bending at the bends radius of 14 mm. (e) The taping experiments setup. (f) Sheet resistance changes with the cycle numbers of taping and peeling.

where *d* is the distance between two clamps, *L* is the length of the electrode, and *r* is the bending radius. A repeated fatigue bending test showed that the flexible electrode maintained its performance even after bending 1000 times to a radius of 14 mm (Figure 4c,d). A fresh 3 M tape (Scotch Magic 810 tape) was attached to a 2.54 × 2.54 cm transparent electrode and then was peeled off by hand. (Figure 4e,f and SI Video 1) The resistance of the electrode was monitored throughout the taping and peeling process. The results (Figure 4f and SI Video 1) indicated that there was no obvious change on the resistance of the electrode after 50 cycles of taping and peeling. As far as we know, such an excellent adhesion is only available with commercial ITO.

The toughness and high performance of the new transparent electrode make it useful in many optoelectronics applications. The compatibility, low fabrication cost and high manufacturing throughput make it a promising method to produce large are transparent electrodes. Flexible transparent electrodes (6 × 6 cm) were fabricated (Figure 3c) and were used to make resistive touch screen devices. (SI Video 2) The transfer-free procedure eliminates protruding

spots, which is very important for thin film devices like touch screens. This protruding-free film is confirmed by both AFM experiment (SI Figure S7) and smooth touch screen writing experience (SI Figure S8c, SI Video 2). The transparent electrode fabrication process can be easily integrated with electric circuit patterning as shown in the Supporting Information (SI Figure S8), which simplifies fabrication for many applications.

CONCLUSION

In this work, a tough and high performance transparent electrode was fabricated by using electrospun fiber as mask pattern. The patterning method is cost-effective and produces large area per unit time. The reported fabrication procedure is free of the transfer step that complicates many other metal nanowires, CNT, or graphene-based transparent electrodes. The protruding spots do not occur on the transparent electrode. The transparent electrodes have a sheet resistance of 6 Ω/□ at 83% transmittance or 24 Ω/□ at 92% transmittance. The fabrication method works well with both rigid glass substrates and flexible PET

substrates. The resulting transparent electrodes show excellent adhesion and bending. A touch screen device based on the flexible transparent electrode was demonstrated.

METHODS

Materials. Polyacrylonitrile powder with molecular weight 150 000 was purchased from Scientific Polymer, Inc. Iron(III) chloride ($FeCl_3$, 98%) powder was purchased from Alfa Aesar. Dimethylformamide (DMF, 99.8%) was received from EMD chemicals Inc. Copper (99.99%) was received from IAmaterials. Aluminum oxide (99.99%) was received from Kamis.

Preparation of Cu Nanowire Electrode. For the metal film deposition, 2 nm Al_2O_3 and copper with different thickness (100 or 50 nm on glass and 60 nm on PET in this work) were deposited by electron-beam deposition using a customized Denton e-beam evaporator under a pressure of 2×10^{-5} Torr. Polyacrylonitrile solution (12 wt % PAN) was prepared by adding polymer powder to dimethylformamide (DMF). The solution was stirred in a water bath at 80 °C for 2 h to ensure the complete dissolution of solid polymer. A voltage of 6 kV and a positive pressure of 27 KPa were applied to the solution to spin the fibers out of a glass capillary with an outer diameter of 0.5 mm. The copper-coated substrates were placed under the capillary to collect PAN fibers. The nanofibers were collected in 30 s. The distance from the capillary tip to the sample surface was 12 cm. The electrospun PAN nanofibers on the substrates were solvent annealed by the setup illustrated in SI Figure S1: A compressed air stream was passed through a hot DMF container (75 °C) to the neck of a funnel. The sample was supported at the mouth of the funnel for 1−3 min. The copper was etched by rinsing it on a holder and was rinsed serially with 1 L of 0.003 M $FeCl_3$ aqueous solution followed by 1 L of 0.0015 M $FeCl_3$ aqueous solution (see SI Figure S2). In the final step, the PAN nanofibers were removed by immersing the sample into hot DMF (50 °C) for 3 min.

Characterization. The sheet resistances of the films were measured using a digital Keithley 2000 multimeter with a Pro-4 Lucas Lab four-point probe to eliminate contact resistance. Ten randomly selected points on each 2.54 × 2.54 cm sample were measured. Both the mean value and standard deviation was reported in Figure 3d. The optical transmittance was obtained by using a Cary 100Bio UV−visible spectrophotometer. The optical images were taken with an Olympus DP70 optical microscope. SEM images were collected with a JEOL JSM-7401 field emission SEM.

Conflict of Interest: The authors declare the following competing financial interest(s): Y.Z. and T.H. are coinventors on provisional patent application (USPTO S/N 61/928,019, Transparent Electrode Prepared by Electrospin Patterning) owned by University of Akron.

Supporting Information Available: The detailed solvent annealing and rinsing etching process, the SEM EDAX images, transparency control experiments, detailed resistive touch screen fabrication process, and the videos of taping/peeling test and touch screen demo. This material is available free of charge *via* the Internet at http://pubs.acs.org.

REFERENCES AND NOTES

1. Kirchmeyer, S.; Reuter, K. Scientific Importance, Properties and Growing Applications of Poly(3,4-Ethylenedioxythiophene). *J. Mater. Chem.* **2005**, *15*, 2077–2088.
2. Cai, W.; Zhu, Y.; Li, X.; Piner, R. D.; Ruoff, R. S. Large Area Few-Layer Graphene/Graphite Films as Transparent Thin Conducting Electrodes. *Appl. Phys. Lett.* **2009**, *95*, 123115.
3. Kim, K. S.; Zhao, Y.; Jang, H.; Lee, S. Y.; Kim, J. M.; Kim, K. S.; Ahn, J. H.; Kim, P.; Choi, J. Y.; Hong, B. H. Large-Scale Pattern Growth of Graphene Films for Stretchable Transparent Electrodes. *Nature* **2009**, *457*, 706–710.
4. Weiss, N. O.; Zhou, H.; Liao, L.; Liu, Y.; Jiang, S.; Huang, Y.; Duan, X. Graphene: An Emerging Electronic Material. *Adv. Mater.* **2012**, *24*, 5782–5825.
5. Zhang, D.; Ryu, K.; Liu, X.; Polikarpov, E.; Ly, J.; Tompson, M. E.; Zhou, C. Transparent, Conductive, and Flexible Carbon Nanotube Films and Their Application in Organic Light-Emitting Diodes. *Nano Lett.* **2006**, *6*, 1880–1886.
6. Hecht, D. S.; Hu, L.; Irvin, G. Emerging Transparent Electrodes Based on Thin Films of Carbon Nanotubes, Graphene, and Metallic Nanostructures. *Adv. Mater.* **2011**, *23*, 1482–1513.
7. Miller, M. S.; O'Kane, J. C.; Niec, A.; Carmichael, R. S.; Carmichael, T. B. Silver Nanowire/Optical Adhesive Coatings as Transparent Electrodes for Flexible Electronics. *ACS Appl. Mater. Interfaces* **2013**, *5*, 10165–10172.
8. Kim, T.; Canlier, A.; Kim, G. H.; Choi, J.; Park, M.; Han, S. M. Electrostatic Spray Deposition of Highly Transparent Silver Nanowire Electrode on Flexible Substrate. *ACS Appl. Mater. Interfaces* **2013**, *5*, 788–794.
9. Leem, D. S.; Edwards, A.; Faist, M.; Nelson, J.; Bradley, D. D.; de Mello, J. C. Efficient Organic Solar Cells with Solution-Processed Silver Nanowire Electrodes. *Adv. Mater.* **2011**, *23*, 4371–4375.
10. Wu, H.; Hu, L.; Rowell, M. W.; Kong, D.; Cha, J. J.; McDonough, J. R.; Zhu, J.; Yang, Y.; McGehee, M. D.; Cui, Y. Electrospun Metal Nanofiber Webs as High-Performance Transparent Electrode. *Nano Lett.* **2010**, *10*, 4242–4248.
11. Guo, H.; Lin, N.; Chen, Y.; Wang, Z.; Xie, Q.; Zheng, T.; Gao, N.; Li, S.; Kang, J.; Cai, D.; et al. Copper Nanowires as Fully Transparent Conductive Electrodes. *Sci. Rep.* **2013**, *3*, 2323.
12. Hu, L.; Kim, H. S.; Lee, J. Y.; Peumans, P.; Cui, Y. Scalable Coating and Properties of Transparent, Flexible, Silver Nanowire Electrodes. *ACS Nano* **2010**, *4*, 2955–2963.
13. Chen, T. L.; Ghosh, D. S.; Mkhitaryan, V.; Pruneri, V. Hybrid Transparent Conductive Film on Flexible Glass Formed by Hot-Pressing Graphene on a Silver Nanowire Mesh. *ACS Appl. Mater. Interfaces* **2013**, *5*, 11756–11761.
14. Zhu, Y.; Sun, Z.; Yan, Z.; Jin, Z.; Tour, J. M. Rational Design of Hybrid Graphene Films for High-Performance Transparent Electrodes. *ACS Nano* **2011**, *5*, 6472–6479.
15. Kholmanov, I. N.; Magnuson, C. W.; Aliev, A. E.; Li, H.; Zhang, B.; Suk, J. W.; Zhang, L. L.; Peng, E.; Mousavi, S. H.; Khanikaev, A. B.; et al. Improved Electrical Conductivity of Graphene Films Integrated with Metal Nanowires. *Nano Lett.* **2012**, *12*, 5679–5683.
16. Chen, R.; Das, S. R.; Jeong, C.; Khan, M. R.; Janes, D. B.; Alam, M. A. Co-Percolating Graphene-Wrapped Silver Nanowire Network for High Performance, Highly Stable, Transparent Conducting Electrodes. *Adv. Funct. Mater.* **2013**, *23*, 5150–5158.
17. Bolotin, K. I.; Sikes, K. J.; Jiang, Z.; Klima, M.; Fudenberg, G.; Hone, J.; Kim, P.; Stormer, H. L. Ultrahigh Electron Mobility in Suspended Graphene. *Solid State Commun.* **2008**, *146*, 351–355.
18. Nair, R. R.; Blake, P.; Grigorenko, A. N.; Novoselov, K. S.; Booth, T. J.; Stauber, T.; Peres, N. M.; Geim, A. K. Fine Structure Constant Defines Visual Transparency of Graphene. *Science* **2008**, *320*, 1308.
19. Novoselov, K. S.; Geim, A. K.; Morozov, S. V.; Jiang, D.; Zhang, Y.; Dubonos, S. V.; Grigorieva, I. V.; Firsov, A. A. Electric Field Effect in Atomically Thin Carbon Films. *Science* **2004**, *306*, 666–669.
20. Eda, G.; Fanchini, G.; Chhowalla, M. Large-Area Ultrathin Films of Reduced Graphene Oxide as a Transparent and

Flexible Electronic Material. *Nat. Nanotechnol.* **2008**, *3*, 270–274.

21. Bae, S.; Kim, H.; Lee, Y.; Xu, X.; Park, J. S.; Zheng, Y.; Balakrishnan, J.; Lei, T.; Kim, H. R.; Song, Y. I.; *et al.* Roll-to-Roll Production of 30-Inch Graphene Films for Transparent Electrodes. *Nat. Nanotechnol.* **2010**, *5*, 574–578.

22. Kim, K. K.; Reina, A.; Shi, Y.; Park, H.; Li, L. J.; Lee, Y. H.; Kong, J. Enhancing the Conductivity of Transparent Graphene Films *via* Doping. *Nanotechnology* **2010**, *21*, 285205.

23. Gunes, F.; Shin, H. J.; Biswas, C.; Han, G. H.; Kim, E. S.; Chae, S. J.; Choi, J. Y.; Lee, Y. H. Layer-by-Layer Doping of Few-Layer Graphene Film. *ACS Nano* **2010**, *4*, 4595–4600.

24. Wu, H.; Kong, D.; Ruan, Z.; Hsu, P. C.; Wang, S.; Yu, Z.; Carney, T. J.; Hu, L.; Fan, S.; Cui, Y. A Transparent Electrode Based on a Metal Nanotrough Network. *Nat. Nanotechnol.* **2013**, *8*, 421–425.

25. Lee, J. Y.; Connor, S. T.; Cui, Y.; Peumans, P. Solution-Processed Metal Nanowire Mesh Transparent Electrodes. *Nano Lett.* **2008**, *8*, 689–692.

26. Zeng, X.-Y.; Zhang, Q.-K.; Yu, R.-M.; Lu, C.-Z. A New Transparent Conductor: Silver Nanowire Film Buried at the Surface of a Transparent Polymer. *Adv. Mater.* **2010**, *22*, 4484–4488.

27. Li, H.; Pan, W.; Zhang, W.; Huang, S.; Wu, H. Tin Nanofibers: A New Material with High Conductivity and Transmittance for Transparent Conductive Electrodes. *Adv. Funct. Mater.* **2013**, *23*, 209–214.

28. Chou, S. Y.; Krauss, P. R.; Renstrom, P. J. Imprint Lithography with 25-Nanometer Resolution. *Science* **1996**, *272*, 85–87.

29. Reneker, D. H.; Yarin, A. L. Electrospinning Jets and Polymer Nanofibers. *Polymer* **2008**, *49*, 2387–2425.

30. Li, X. S.; Zhu, Y. W.; Cai, W. W.; Borysiak, M.; Han, B. Y.; Chen, D.; Piner, R. D.; Colombo, L.; Ruoff, R. S. Transfer of Large-Area Graphene Films for High-Performance Transparent Conductive Electrodes. *Nano Lett.* **2009**, *9*, 4359–4363.

31. Yan, Z.; Lin, J.; Peng, Z.; Sun, Z.; Zhu, Y.; Li, L.; Xiang, C.; Samuel, E. L.; Kittrell, C.; Tour, J. M. Toward the Synthesis of Wafer-Scale Single-Crystal Graphene on Copper Foils. *ACS Nano* **2012**, *6*, 9110–9117.

32. Sigma-Aldrich. http://www.sigmaaldrich.com/united-states.html, accessed on December 9, 2013.

33. Hu, L.; Hecht, D. S.; Gruner, G. Percolation in Transparent and Conducting Carbon Nanotube Networks. *Nano Lett.* **2004**, *4*, 2513–2517.

34. De, S.; Coleman, J. N. The Effects of Percolation in Nanostructured Transparent Conductors. *MRS Bull.* **2011**, *36*, 774–781.